The Effect of Calcium Oxide Addition on the Removal of Metal Impurities from Metallurgical-Grade Silicon by Acid Leaching

FALIN HE, SONGSHENG ZHENG, and CHAO CHEN

The removal of metal impurities from metallurgical grade silicon (MG-Si) by acid leaching has been investigated with the addition of CaO. Prior to adding CaO, Fe is the main impurity in the MG-Si sample, and the 2nd-phase precipitates in silicon are Si-Fe-based alloys, such as Si-Fe, Si-Fe-Ti, Si-Fe-Al, Si-Fe-Mn, and Si-Fe-Ni. The phases of Si-Fe and Si-Fe-Ti are not appreciably soluble in HCl. After the introduction of CaO, Ca becomes the dominant impurity, and the 2nd-phase precipitates become Si-Fe-based alloys, such as Si-Ca, Si-Ca-(Fe, Ti, Ni, Al), and Si-Ca-Fe-Al. These are effectively leached with HCl. Therefore, the HCl leaching effect on the removal of metal impurities has been improved. The optimum content of Ca in the MG-Si samples after adding CaO is in the range of 1 pct to 4 pct, the contents of Fe, Al, Ti, and Ni have been decreased to a minimum of less than 5 ppmw (ppm by weight) each, and the acid leaching results do not show a dependence on Ca content at this range.

DOI: 10.1007/s11663-012-9681-z

I. INTRODUCTION

SOLAR energy will shortly be in great demand because it is inexhaustible and cleaner than any conventional energy resources. Because of the energy crisis and the greenhouse warming, the photovoltaic (PV) industry has grown up rapidly. According to the EPIA annual report,[1] the PV market has continued to grow by almost 15 pct in 2009 compared with that in 2008, and the total power capacity installed in the world has risen by 45 pct up to 22.9 GW.

Silicon is one of the main substrate materials for solar cells. The purity requirement of solar grade silicon (SoG-Si) is less than that of electronic-grade silicon (EG-Si). Currently, the expensive ultrahigh-purity EG-Si has been used to produce solar cells at a prohibitive price. One alternative was to use less expensive "scrap" or off-specification supply of EG-Si from the semiconductor industry. However, the improvements in silicon clip productivity have resulted in a decrease in the "scrap" supply of electronic-grade silicon. With the growth of PV industry, it seems inevitable to create an independent feedstock supply for SoG-Si. Extensive attention and development have been focused on metallurgical processes. Wolf *et al.*[2] succeeded in producing solar cells with the conversion efficiency of 12.38 pct, which was made from SoG-Si obtained by metallurgical processing. Ciszek *et al.*[3] reported a new approach for producing SoG-Si from metallurgical-grade silicon (MG-Si). The approach was based on atmospheric pressure iodine vapor transport, where the small CZ crystals with resistivity of approximately 0.4 ohm-cm has been grown, but boron and phosphorus were both presented in relatively large quantities in the CZ crystals. As a result, the solar cell only had a low efficiency of 9.5 pct and a low minority carrier diffusion length of 8 μm. In the industry, companies such as Elkem (Oslo, Norway), Ferro Atlantica (Medina, OH), and Dow Corning (Midland, MI) have been working on producing SoG-Si from MG-Si by metallurgical processes.[4] Elkem announced that the energy consumption of their metallurgical processes was approximately 15 kwh/kg by implementing slag refining and acid/alkaline surface treatment, and the solar cells produced from this kind of SoG-Si had an efficiency of 15 to 16 pct.

The total metal impurities content in MG-Si is approximately 1 to 2 pct by mass. MG-Si can be purified by different metallurgical processes, including acid leaching, Si-Al alloy processing, directional solidification, vacuum refining, slag treatment, gas blowing, plasma purification, electron beam melting, and so on.[5] The acid leaching treatment is one of the most efficient processes for the removal of metal impurities. Chu *et al.*[6] carried out the acid leaching process by refluxing pulverized MG-Si of undefined grain size with aqua regia for 100 hours, and more than 80 pct of metal impurities was removed. Voos[7] claimed in his patented process that H_2SO_4, aqua regia, HF, and other acids have been used to treat MG-Si with the average particle size less than 50 μm, and the purity of the silicon obtained was available for microwave diodes application. Dietl[8] reported that the best elimination results for most impurities were achieved by soaking MG-Si powder in an aqueous solution of hydrochloric acid and hydrofluoric acid. Norman *et al.*[9] obtained 99.9 pct Si by leaching in three successive steps with

FALIN HE, Ph.D. Student, is with the College of Physics and Mechanics and Electrics, Xiamen University, 361005 Xiamen, P.R. China. SONGSHENG ZHENG, Assistant Professor, is with the School of Energy Research, Xiamen University. CHAO CHEN, Professor, is with the College of Physics and Mechanics and Electrics, Xiamen University, and also with the School of Energy Research, Xiamen University. Contact e-mail: cchen@xmu.edu.cn

Manuscript submitted September 26, 2011.
Article published online June 29, 2012.

aqua regia, hydrofluoric acid, and hydrochloric acid. Juneja and Mukherjee[10] reported that the enabling production of 99.95 pct Si was obtained from 150 μm MG-Si by use of hydrofluoric acid at 323 K (50 °C). Shimpo *et al.*[11] presented that 80.4 pct of phosphorus were removed when the concentration of calcium was 5.13 pct. Yu *et al.*[12] confirmed that, 85 pct of Fe and 75 pct of Al were removed by immersing MG-Si powder into acid for 4 days, where an acid named as C with a temperature of 333 K (60 °C) and MG-Si powder with particles size of 50 μm have been used. Hunt et al.[13,14] reported that more than 90 pct impurities were dissolved by immersing MG-Si in aqua regia for 12 hours at 348 K (75 °C). Despite the good results obtained in the preceding reports, the leaching behavior of different types of MG-Si from different origins is unclear. A similar mechanism of acid leaching on Si-Fe alloy was investigated by Margarido *et al.*[15–19] It has been determined that the 2nd-phase precipitates were a function of the original composition, and the ratios of Fe/Si and Al/Ca had an obvious effect on the rate of alloy dissolution in acid.

In this article, the mechanism of generating silicide in the silicon crystal boundary has been investigated. The variation of precipitation phase in silicon has been observed before and after the addition of CaO to MG-Si. The effects of calcium oxide addition on the removal of metal impurities by acid leaching are also discussed.

II. EXPERIMENTS

A. *Sample Preparation*

The melting experiments were carried out in a laboratory-scale induction furnace. In this furnace, the crucible-coil assembly was positioned approximately at the center of a water-cooled vacuum chamber of 0.5 m diameter and 0.5 m depth. At the beginning, a uniform mixture was prepared by mixing a certain amount of analytical grade CaO powder (99.5 pct CaO) and 100 g MG-Si powder (99.5 pct Si). Then, the mixture was melted in a graphite crucible with an inner diameter of 0.055 m and depth of 0.09 m heated by an induction supply. During the melting, the chamber was filled with Ar gas to 20000 Pa, and the temperature was measured continuously with a two-color optical pyrometer (Marathon MR1S; Raytek Corporation, Santa Cruz, CA). With a continuous temperature measurement and with a manual control of power input to the furnace, the temperature of the melt could be maintained constant at 2073 K (1800 °C [±10 °C]). After being held for 3 hours, the melt was cast into a graphite mold and cooled down. Then, the ingot obtained was longitudinally cut in two pieces. One piece was crushed and ground to 100 to 120 mesh powder, and the powder was analyzed by an inductively coupled plasma optical emission spectrometer (ICP-OES; ELAN 6100; National Thermal Power Corporation/PerkinElmer, Waltham, MA). The other piece was polished on the longitudinal section and analyzed by an electron probe microanalyzer (EPMA; JXA-8100; Japan Electronics Co., Ltd.).

B. *Acid Leaching Treatment*

The acid leaching treatment was done on both the powder and the longitudinal section. The powder with particles of 100 to 120 mesh was put in a poly-tetra-fluoro-ethylene (PTFE) container, and the acid with a certain concentration was continuously added into the container until the powder was immersed, The PTFE container was placed in a 353 K (80 °C) water bath. After a period of time, the powder was washed with deionized water. This process was one cycle of acid leaching. Three cycles of acid leaching were carried out with reagent-grade HCl (4 mol/L), aqua regia (6 mol/L), and HF (1 mol/L) for 24 hours, 12 hours, and 12 hours, respectively. The powder was then rinsed with deionized water and dried. The powder was then analyzed by ICP-OES. The acid leaching treatment on the longitudinal section was only executed in one cycle with HCl for 2 hours, and then the longitudinal section was rinsed, dried, and analyzed by EPMA.

III. RESULTS AND DISCUSSION

A. *MG-Si*

In the solidification process, most of the metal impurities or silicides will segregate in the precipitation phase because of the segregation behavior of impurities in MG-Si. In this article, the segregation coefficient is defined as a ratio of the concentration of an impurity element in the solid phase to that in the liquid phase. Obviously, if the segregation coefficient is less than unity, then the concentration of the impurity in the liquid phase will be larger than that in the solid phase. Moreover, the smaller the segregation coefficient, the more content of the impurity will be segregated in the liquid phase. The standard content of the impurities in MG-Si and SoG-Si together with the corresponding segregation coefficients have been reviewed by Zheng *et al.*[20] as is listed in Table I.

As is shown in Table I, the top three metal impurities in MG-Si are Fe, Al, and Ca, which will be segregated in the grain boundary when the silicon melt is cooled. The precipitate will probably include Si-Fe and Si-Ca binary phases, a Si-Fe-Al ternary phase, and a Si-Fe-Al-Ca quaternary phase.[18] In the current study, the grain boundary on the longitudinal section is scanned by EPMA mapping and shown in Figure 1. The microstructure of the precipitation phase is analyzed by wavelength dispersive X-ray spectroscopy (WDS) and shown in Figure 2.

As shown in Figure 1, the metal impurities of Fe, Al, Ca, Ti, and Ni have uneven distribution in the precipitates, and the oxides of Al and Si have also been observed in the precipitates. In Figure 2, the large light gray area in the precipitates is a Si-Fe binary phase, and the other scattered area is the ternary phase of Si-Fe-M (Al/Ca/Ti/Ni) and quaternary alloy of Si-Fe-Al-Ca. However, the Si-Al binary alloy cannot be observed. The reason is that the melting point of Si-Al-M (Fe/Ca) ternary or quaternary alloy is higher than that of Si-Al binary alloy. Therefore, the Si-Al binary system prefers

Table I. Impurity Content of Metallurgical-Grade Silicon and Solar-Grade Silicon

Impurity	Impurity Content, ppmw			Segregation Coefficient
	Metallurgical Grade			
	98-99 pct	99.50 pct	Solar Grade	
Al	1000 to 4000	50 to 600	<0.1	2.0×10^{-3}
Fe	1500 to 6000	100 to 1200	<0.1	8.0×10^{-6}
Ca	250 to 2200	100 to 300	<1	1.3×10^{-4} to 5.2×10^{-4}
Mg	100 to 400	50 to 70	<1	3.2×10^{-6}
Mn	100 to 400	50 to 100	<<1	1.3×10^{-5}
Cr	30 to 300	20 to 50	<<1	1.1×10^{-5}
Ti	30 to 300	10 to 50	<<1	2.0×10^{-6}
V	50 to 250	<10	<<1	4.0×10^{-6}
Zr	20 to 40	<10	<<1	1.6×10^{-8}
Cu	20 to 40	<10	<1	4.0×10^{-4}
B	10 to 50	10 to 15	0.1 to 1.5	8×10^{-1}
P	20 to 42	10 to 20	0.1 to 1	3.5×10^{-1}
C	1000 to 3000	50 to 100	0.5 to 5	5×10^{-2}

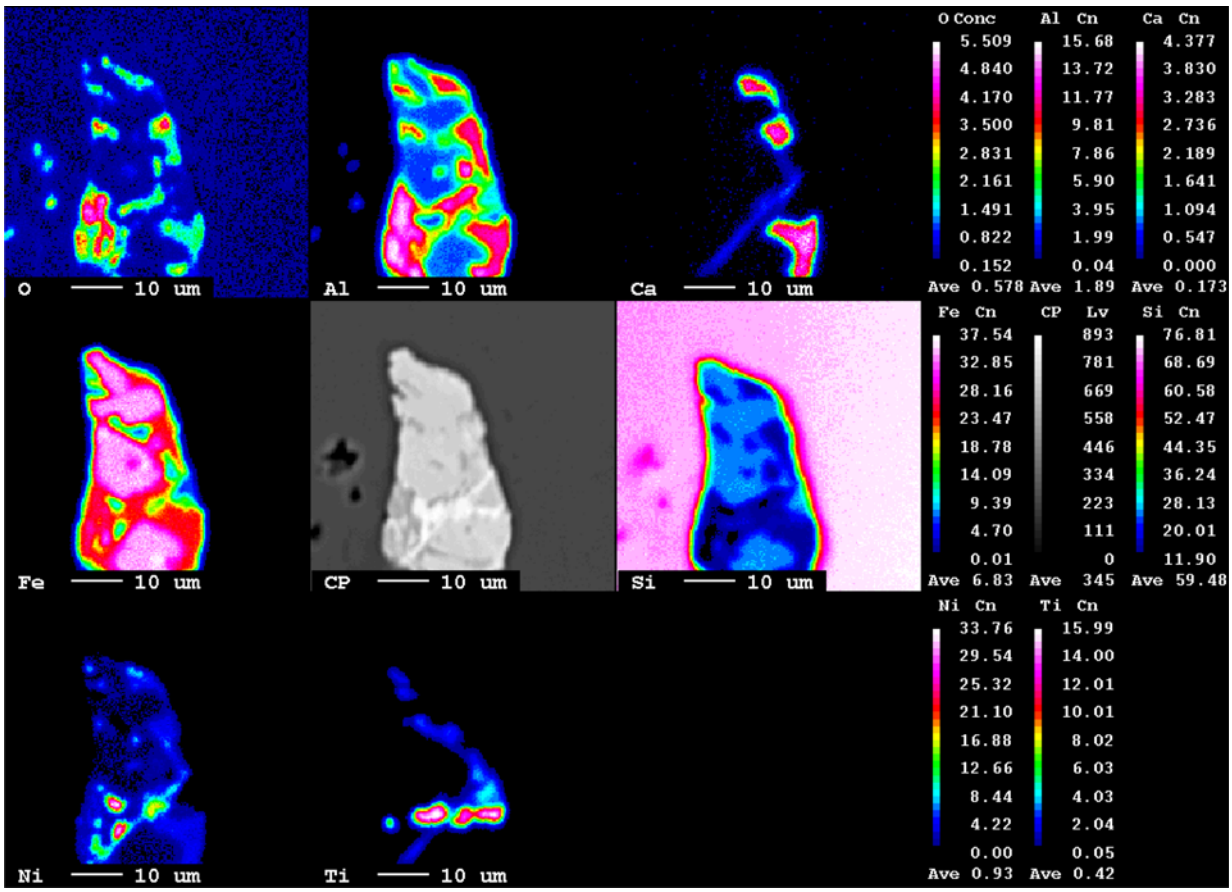

Fig. 1—EPMA mapping of MG-Si.

to catch another one or two elements and form a ternary or quaternary precipitates before the temperature goes down to the melting point of Si-Al binary alloy at 848 K (575 °C).[21]

The contents of metal impurities in the precipitation phase in Figure 2 have been analyzed by EPMA-WDS with 50 pct-70 pct Si, 20 pct-40 pct Fe, 5 pct-10 pct Al, 5 pct-10 pct Ti, and 1 pct-5 pct Ca.

B. *MG-Si After Adding CaO*

Five samples were prepared by adding CaO into MG-Si, and the calcium content was controlled by adding different amounts of CaO when preparing the different samples. The contents of metal impurities in MG-Si before and after adding different amounts of CaO were analyzed by ICP-OES and are listed in Table II.

Although the addition of CaO in the five samples was changed, the EPMA mapping on the longitudinal section showed no obvious difference on the precipitated species. Therefore, only one EPMA mapping picture was shown in Figure 3, and the corresponding microstructure was shown in Figure 4.

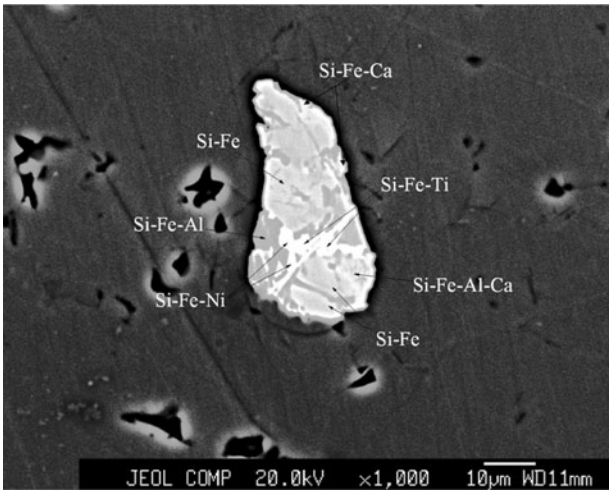

Fig. 2—Microstructure of metal impurities precipitation in MG-Si analyzed by EPMA-WDS.

The contents of metal impurities in the precipitation phase after adding CaO in Figure 4 have been analyzed by EPMA-WDS and are as follows: 40 pct-60 pct Si, 5 pct-20 pct Fe, 0.5 pct-1.0 pct Al, 0.5 pct-1.0 pct Ti, and 20 pct-40 pct Ca. As a comparison of EPMA-WDS analysis on the precipitation phase in Figure 2 and Figure 4, it can be observed that Ca replaces Fe and

Table II. The Content of Metal Impurities in MG-Si Before and After Adding CaO (ppmw)

	Metal Impurities				
Sample	Fe	Al	Ca	Ti	Ni
MG-Si (original)	1400	860	50	12	33
MG-Si-1	1504	748	59627	10	35
MG-Si-2	1457	726	35108	10	33
MG-Si-3	1405	724	21390	9	32
MG-Si-4	1492	740	12470	11	36
MG-Si-5	1427	725	6385	11	35

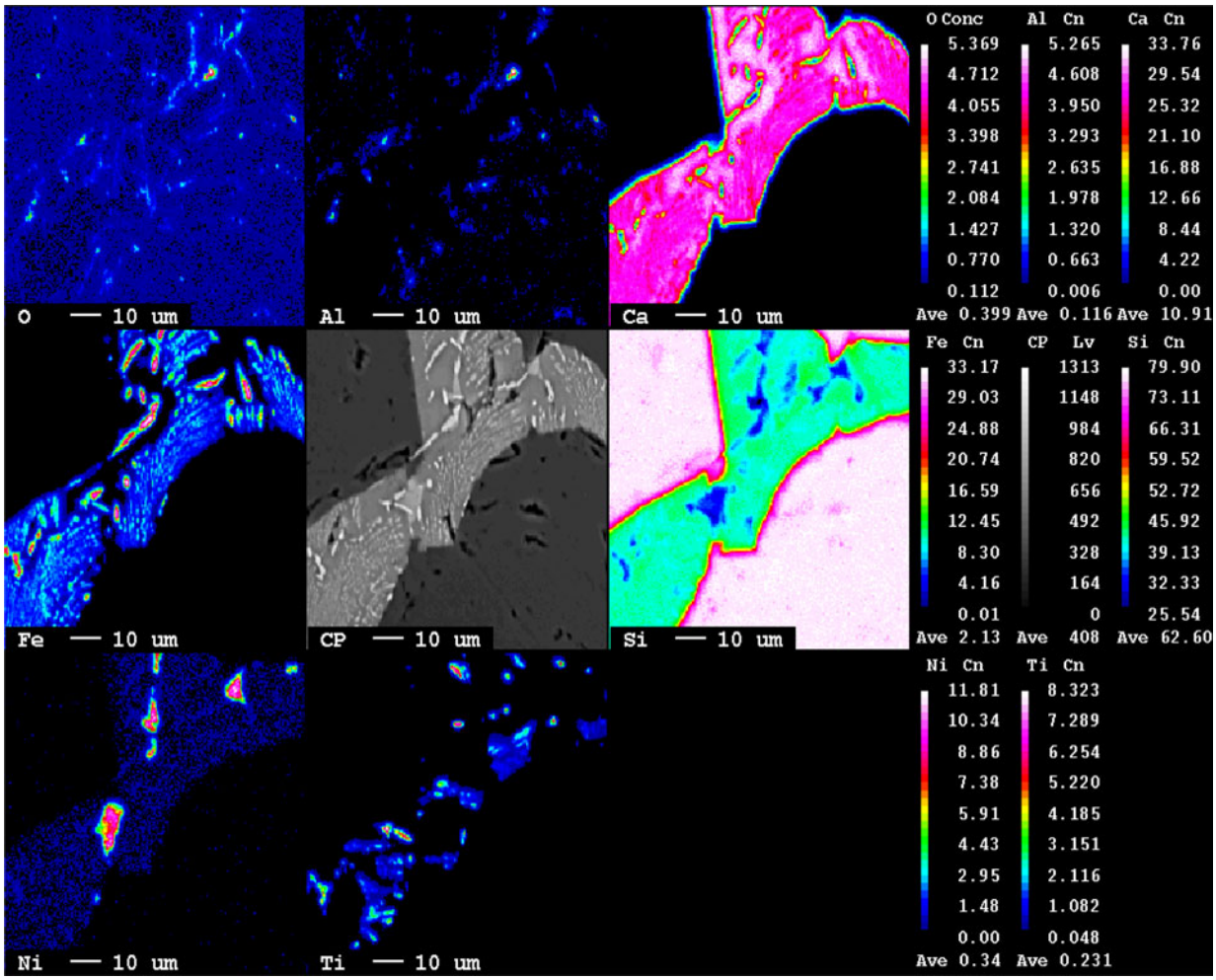

Fig. 3—EPMA mapping of MG-Si after adding CaO.

becomes the dominant impurity in the precipitation phase when CaO is added. As is shown Figures 3 and 4, Si-Ca binary alloy and Si-Ca-Fe (Al/Ni/Ti) ternary phase have been found in the precipitation phase, and the scattered Si-Ca-Fe-Al quaternary phase embedded in precipitation phase has been observed. However, the Si-Fe-base alloys have all disappeared. These phenomena can be explained from the Si-Fe-Ca ternary phase diagram in Figure 5.

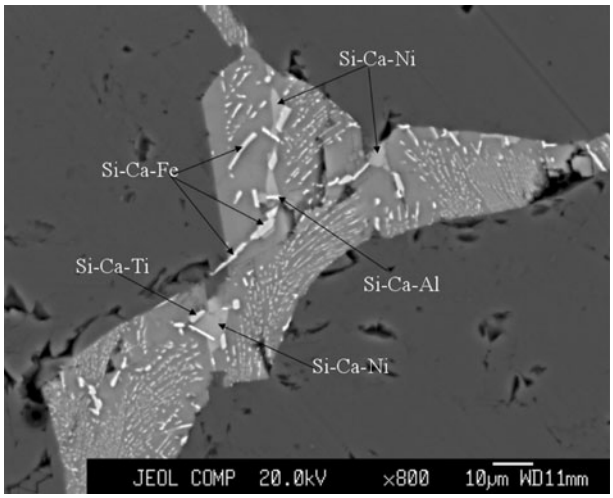

Fig. 4—Microstructure of metal impurities precipitation in MG-Si after adding CaO, analyzed by EPMA-WDS.

As can be observed, the temperature of the ternary phase diagram in Figure 5 is less than 1673 K (1400 °C). At the low Fe side in the phase diagram, the Si-Ca alloy phase will change with decreasing Ca content, such as Ca_2Si (>60 pct Ca), CaSi (40 pct-60 pct Ca), and $CaSi_2$ (>25 pct Ca) in sequence. Similarly, at the low Ca side, the Si-Fe alloy phase will change in descending order by Fe content as Fe_3Si (>80 pct Fe), Fe_2Si (>60 pct Fe), FeSi (40 pct-60 pct Fe), and $FeSi_2$ (>25 pct Fe). Therefore, in the Si-Fe-Ca ternary system, the species of alloy phases depend on the content of Ca and Fe. As is listed in Table II, the main impurity in the sample of MG-Si (original) is Fe, so Si-Fe-base alloys are the main precipitation phase in MG-Si (Figures 1 and 2). When CaO is added to the MG-Si samples (MG-Si-1 to MG-Si-5) in Table II, the contents of Ca increase, and Ca becomes the dominant impurity; thus, the Si-Fe-base precipitates have been replaced by Si-Ca-base alloy phases (Figures 3 and 4).

C. *Acid Leaching of MG-Si*

The microstructure of MG-Si longitudinal section after acid leaching is shown in Figure 6, and the EPMA mapping on the corresponding residue precipitation phase is shown in Figure 7.

By comparing the EPMA analysis results of MG-Si with CaO addition (Figures 6 and 7) with the original MG-Si without CaO addition (Figures 1 and 2), it is clear that the Si-Fe-Ca ternary phase together with Si-Fe-Al-Ca quaternary phase have been etched by HCl.

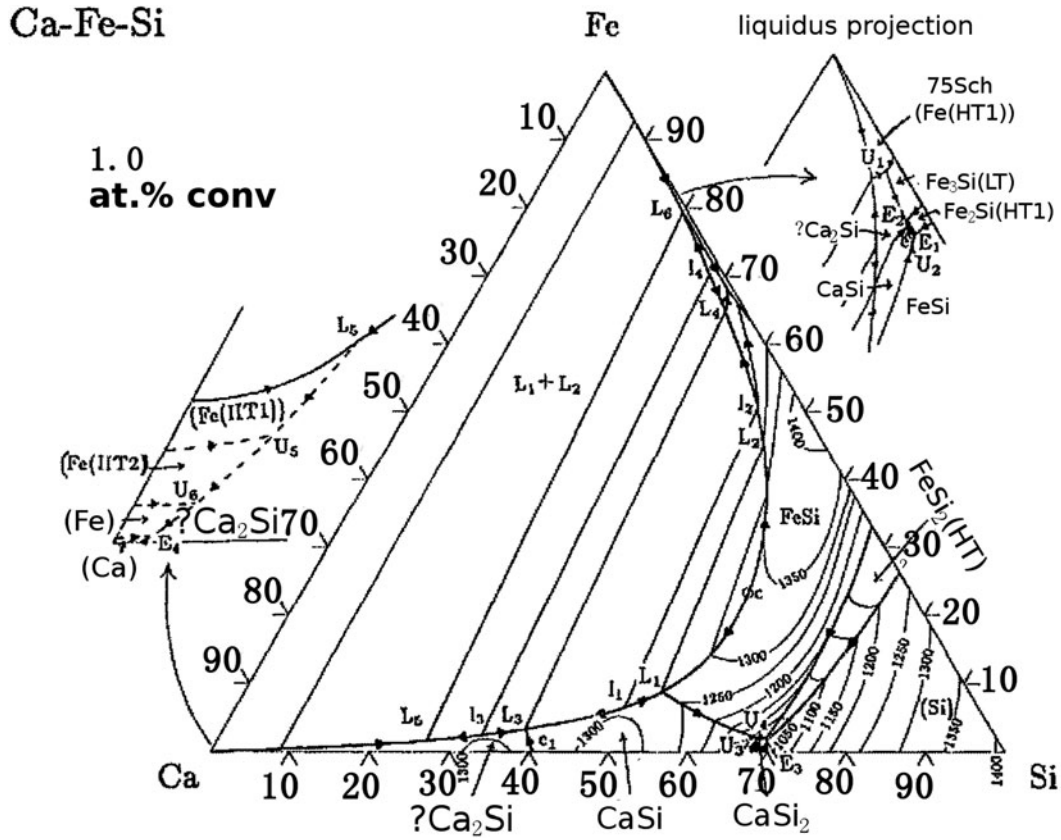

Fig. 5—Si-Fe-Ca ternary phase diagram.

Simultaneously, almost all the oxides are taken away by HCl leaching. However, the large areas of the Si-Fe binary phase and Si-Fe-M (Ti/Ni/Al) ternary phase have no significant reaction with HCl.

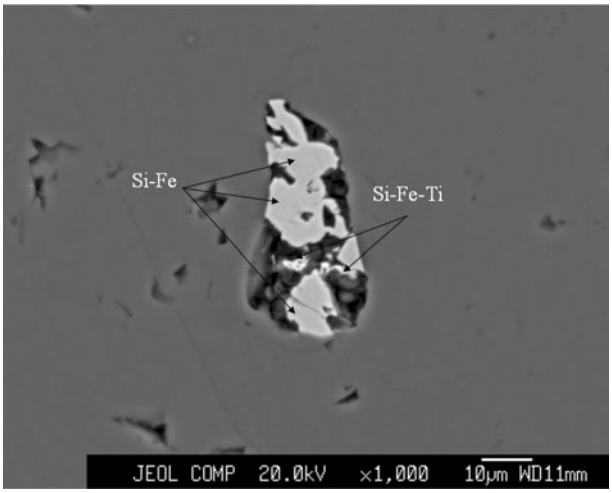

Fig. 6—Microstructure of MG-Si sample after leaching in HCl 4mol/L 353 K (80 °C) 4 h.

D. *Acid Leaching of MG-Si With the Addition of CaO*

The effects of CaO addition on the impurities removal from MG-Si by acid leaching have been evaluated in Figures 8(a) and (b).

After adding CaO, the precipitates have all been changed to Si-Ca alloy or Si-Ca-based alloy (Figure 4). Furthermore, it is determined in Figures 8(a) and (b) that the Si-Ca and the Si-Ca-based precipitates can be effectively removed by HCl leaching.

E. *Comparison of Acid Leaching of MG-Si With and Without the Addition of CaO*

All six MG-Si samples, with or without addition of CaO, were processed by three cycles of acid leaching with HCl, aqua regia, and HF for 24 hours, 12 hours, and 12 hours, respectively. The acid leaching results were analyzed by ICP-OES and are listed in Table III.

As a comparison of the data in Tables II and III, the addition of CaO significantly improved the removal of the metal impurities from MG-Si by HCl. As is shown in Table II, the content of Ca in the MG-Si samples was in the range of 0 pct to 7 pct, and in Table II, the impurities in the samples have all been decreased by acid leaching. Moreover, the contents of Fe, Al, Ti, and

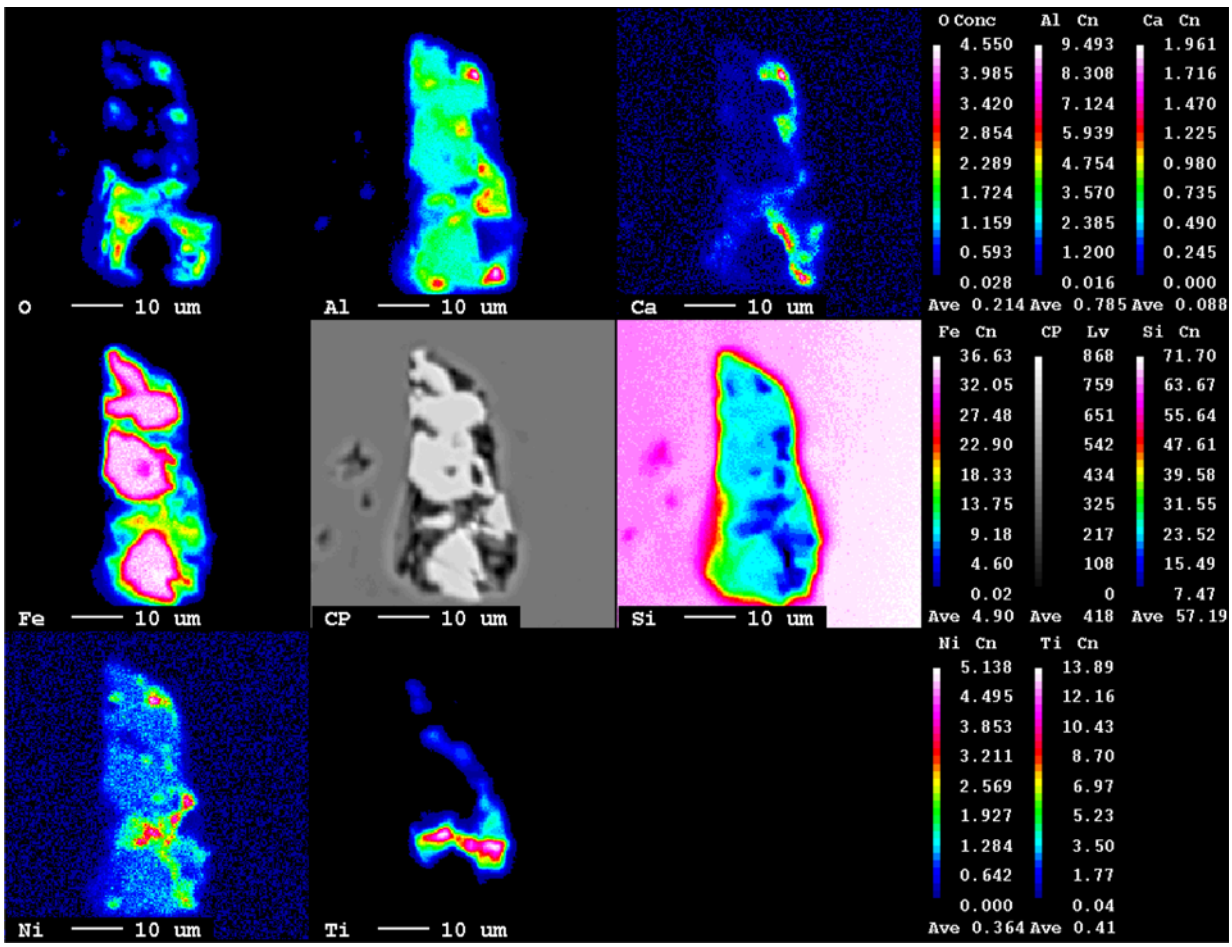

Fig. 7—EPMA mapping of MG-Si sample after leaching in HCl 4 mol/L 353 K (80 °C) 4 h.

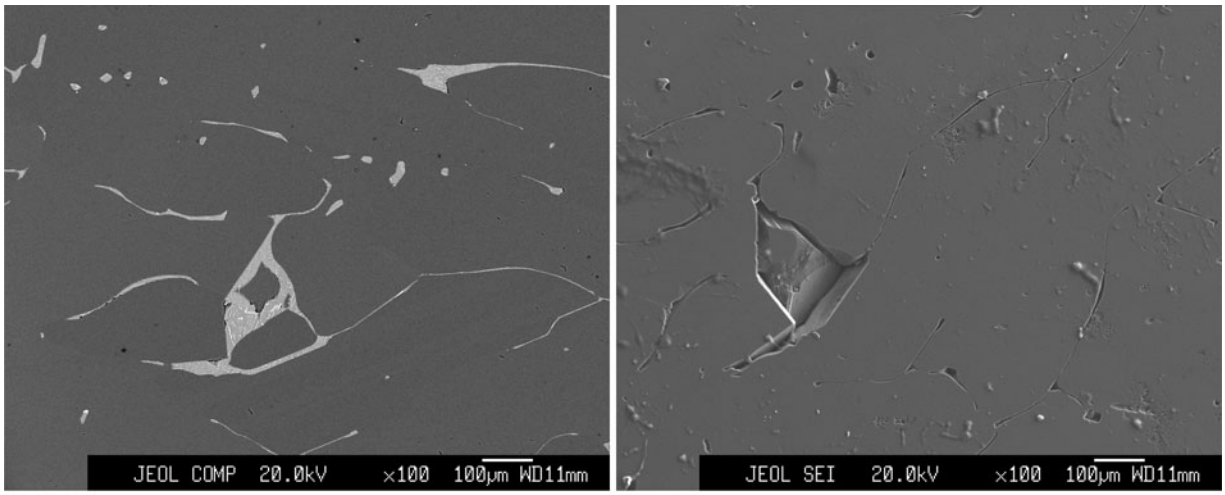

(a) Before leaching (b) After leaching in HCl 4mol/L 353K (80°C) 4 hours

Fig. 8—Microstructure of MG-Si with the addition of CaO.

Table III. Main Impurities Concentration after Acid Leaching of MG-Si (ppmw)

	Metal Impurities				
Sample	Fe	Al	Ca	Ti	Ni
MG-Si (original)	60	68	3	10	27
MG-Si-1	4	2	427	8	3
MG-Si-2	4	3	110	5	3
MG-Si-3	13	4	56	5	4
MG-Si-4	11	15	25	5	4
MG-Si-5	43	58	21	9	20

Ni decreased to a minimum of less than 5 ppmw (ppm by weight) in the sample MG-Si-2. In addition, there was no significant difference of impurities elimination among the samples of MG-Si-1 to MG-Si-4 with different content of Ca. However, the worst acid leaching result was obtained in the sample MG-Si-5 whose Ca content of was approximately 0.6 pct mass. Therefore, the optimum content of Ca in MG-Si was in the range of 1 to 4 pct.

Theoretically, the precipitates in the original MG-Si are Si-Fe-based alloy phases when Fe is the main impurity. With the addition of CaO to MG-Si, Ca will replace Fe and will become the dominant impurity in the precipitate. Consequently, the precipitate changes from HCl insoluble Si-Fe-based alloy phases to HCl soluble Si-Ca-based alloy phases. Therefore, the HCl leaching effect on the removal of metal impurities has been improved. It has also been determined by Margarido *et al.*[18] in their publication that the reactivity sequences of the alloy phases with HCl are CaSi, CaSi2, CaAl2Si1.5 > Fe-Al-Si-Ca > Al-Fe-Si >> FeSi2.

IV. CONCLUSIONS

In this article, the effects of CaO addition on the removal of metal impurities from MG-Si by acid leaching have been investigated. The following conclusions are made in this article:

1. Fe is the main impurity in the original MG-Si sample used in the current study; therefore, Si-Fe-based alloys such as Si-Fe, Si-Fe-Ti, Si-Fe-Al, Si-Fe-Mn, and Si-Fe-Ni, have been observed in the 2nd-phase precipitates of MG-Si. Among these phases, Si-Fe and Si-Fe-M (Ti/Ni/Al) are nearly insoluble in HCl.
2. After introduction of CaO to MG-Si, Ca becomes the dominant impurity in the samples. The precipitates change from acid insoluble Si-Fe-based to acid soluble Si-Ca-based alloys, such as Si-Ca, Si-Ca-M (Fe/Ti/Ni/Al), and Si-Ca-Fe-Al. Therefore, the HCl leaching effect on the removal of the metal impurities has been improved.
3. The optimum content of Ca in MG-Si samples after adding CaO is in the range of 1 to 4 pct. The acid leaching results do not show a dependence on Ca content at this range.

REFERENCES

1. E. Despotou, A.E. Gammal, B. Fontaine, D.F. Montoro, M. Latour, S. Lenoir, G. Masson, P. Philbin, and P.V. Buggenhout: *Market Outlook for Photovoltaics Until 2014*, EPIA, Brussels, Belgium, 2010.
2. S.D. Wolf, J. Szlufcik, Y. Szlufcik, Y. Delannoy, I. Péchaud, C. Häßler, and R. Einhaus: *Sol. Energ. Mater. Sol. Cell.*, 2002, vol. 72, pp. 49–58.
3. T.F. Ciszek, T.H. Wang, M.R. Page, R.E. Bauer, and M.D. Landry: *Solar-Grade Silicon from Metallurgical-Grade Silicon via Iodine Chemical Vapor Transport Purification*, National Renewable Energy Laboratory, Golden, CO, 2002.
4. E. Øvrelid, B. Geerligs, A. Wærnes, O. Raaness, I. Solheim, R. Jensen, K. Tang, S. Santeen, and B. Wiersma: *Silicon Chem. Indus.*, 2006, vol. 8, pp. 12–16.
5. A. Ciftja, T.A. Engh, and M. Tangstad: *Refining and Recycling of Silicon: A Review*, NTNU, Trondheim, Norway, 2008, pp. 3–20.
6. T.L. Chu and S. Chu: *J. Electro. Chem. Soc.*, 1983, vol. 130, pp. 455–57.
7. W. Voos: U.S. Patent 2,972,521, 1961.
8. J. Dietl: *Sol. Cell.*, 1983, vol. 10, pp. 145–54.

9. C.E. Norman, R.E. Thomas, and E.M. Absi: *Can. J. Phys.*, 1983, vol. 63, pp. 859–62.
10. J.M. Juneja and T.K. Mukherjee: *Hydrometallurgy*, 1986, vol. 16, pp. 69–75.
11. T. Shimpo, T. Yoshikawa, and K. Morita: *Metall. Mater. Trans. B*, 2004, vol. 35B, pp. 277–84.
12. Z. Yu, W. Ma, Y. Dai, B. Yang, C. Liu, P. Dai, and X. Wang: *Trans. Nonferrous Met. Soc. China*, 2007, vol. 17, pp. 1030–33.
13. L.P. Hunt, V.D. Dosaj, J.R. Mccormick, and L.D. Crossman: *Record of the 12th IEEE Photovoltaic Specialists Conf.*, 1976, pp. 125–29.
14. L.P. Hunt, V.D. Dosaj, J.R. Mccormick, and L.D. Crossman: *Solar Energy, Proc. Int. Symp. Electrochem. Soc*, J.B. Borkowitz and I.A. Lask, eds., New York, NY, 1976, pp. 200–15.
15. F. Margarido, J.P. Martins, M.O. Figueiredoc, and M.H. Bastos: *Hydrometallurgy*, 1993, vol. 34, pp. 1–11.
16. F. Margarido, J.P. Martins, M.O. Figueiredoc, and M.H. Bastos: *Hydrometallurgy*, 1993, vol. 32, pp. 1–8.
17. F. Margarido, M.O. Figueiredo, and J.P. Martins: *Mater. Chem. Phys.*, 1994, vol. 38, pp. 342–47.
18. F. Margarido, M.O. Figueiredo, A.M. Queiroz, and J.P. Martins: *Ind. Eng. Chem. Res.*, 1997, vol. 36, pp. 5291–95.
19. A.M. Queiroz, F. Margarido, and M.O. Figueiredo: *Mineral Process: Extractive Metall. Rev. Int. J.*, 2001, vol. 22, pp. 303–22.
20. S. Zheng, J. Safarian, S. Seok, S. Kim, T. Merete, and X. Luo: *Trans. Nonferrous Met. Soc. China*, 2011, vol. 21, pp. 697–702.
21. T. Margria, J.C. Anglezio, and C. Servant: *Ferroalloys*, 1994, vol. 5, pp. 43–48.